Title	Temporal coupled-mode theory of ring–bus–ring Mach–Zehnder interferometer
Author(s)	Zhang, Yanbing; Mei, Ting; Zhang, Dao Hua
Citation	Zhang, Y., Mei, T., & Zhang, D. H. (2012). Temporal coupled-mode theory of ring–bus–ring Mach–Zehnder interferometer. Applied Optics, 51(4), 504-508.
Date	2012
URL	http://hdl.handle.net/10220/10095
Rights	© 2012 Optical Society of America. This paper was published in Applied Optics and is made available as an electronic reprint (preprint) with permission of Optical Society of America. The paper can be found at the following official DOI: [http://dx.doi.org/10.1364/AO.51.000504]. One print or electronic copy may be made for personal use only. Systematic or multiple reproduction, distribution to multiple locations via electronic or other means, duplication of any material in this paper for a fee or for commercial purposes, or modification of the content of the paper is prohibited and is subject to penalties under law.

Temporal coupled-mode theory of ring–bus–ring Mach–Zehnder interferometer

Yanbing Zhang,[1] Ting Mei,[2,*] and Dao Hua Zhang[1]

[1]Department of Electric and Electronic Engineering, Nanyang Technological University, 50 Nanyang Avenue, 639798, Singapore

[2]Institute of Optoelectronic Materials and Technology, South China Normal University, Guangzhou 510631, China

*Corresponding author: ting.mei@ieee.org

Received 10 August 2011; revised 22 October 2011; accepted 28 October 2011;
posted 31 October 2011 (Doc. ID 152526); published 27 January 2012

The temporal coupled-mode theory (TCMT) for a ring–bus–ring Mach–Zehnder interferometer device is developed by taking energy conservation into account. The intercavity interaction in the device is facilitated via a tricoupler, which makes the decay of modes quantitatively different from that in other existing resonator schemes. The TCMT is related to the transfer matrix formalism with energy conservation and the Q factor, and it predicts results in good agreement with the experimental results. The mode analysis from the TCMT is quite illustrative because it can mimic the transparency as an electromagnetically induced transparency expression. The analysis of the tricoupler is applicable for analyzing the transparent resonance in two other similar configurations.

OCIS codes: 130.3120, 140.4780, 130.4815, 230.4555.

1. Introduction

Temporal coupled-mode theory (TCMT) is a promising approach to revealing the work mechanisms of resonators because it gives analysis to the time-dependent behavior between the incident/transmitted waves and resonant modes using time differential equations [1]. The dynamic equation has been tremendously successful in modeling a wide variety of passive and active optical resonant devices [2–6]. In these structures, the resonators are typically loaded with one or several incoming/outgoing ports to allow frequency-selective power transfer between the ports. In the case when only a single mode is presented in the lossless cavities, mode coupling between the bus and cavities can be described by a unitary S matrix, which is derived from the standard TCMT [7]. However, when more than one resonant mode is presented, it is possible that the optical modes inside the resonators can only be described using a nonorthogonal basis function [8]. The presence of such nonorthogonality introduces interesting effects on the transmission behaviors of multimode cavities. For example, an induced transparency in the transmission spectrum resembling an atomic electromagnetically induced transparency (EIT) can be achieved in a structure with a middle waveguide sandwiched by two side-coupled photonic crystal (PhC) cavities [8]. This induced transparency can be used for all-optical dynamical storage of light in the solid-state [3,4] and high-performance modulator [9]. However, in the above examples, most devices are based on the 2×2 coupler, but few are based on the 3×3 coupler (tricoupler) [10]. In our previous work [11,12], the transfer matrix formalism (TMF) was developed to investigate a ring–bus–ring Mach–Zehnder interferometer (RBR-MZI) (see Fig. 1), where the resonant modes interact with each other at the tricoupler, demonstrating the capability of generating EIT-like transparent spectra in such a device.

In this paper, we further our investigation by applying TCMT to illustrate the transparency property of the RBR-MZI device intuitively and show a good agreement is reached between the two theoretical analyses (TMF and TCMT) and experimental observations. The upper MZI arm in Fig. 1 depicts the schematic of a RBR resonator in this device, which consists of two rings, R1 and R2, with single modes

1559-128X/12/040504-05$15.00/0

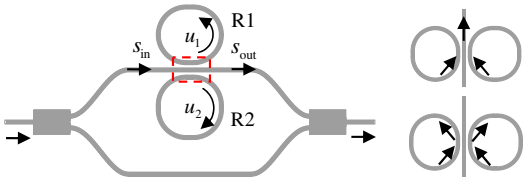

Fig. 1. (Color online) Schematic of the RBR-MZI. The insets present the two characteristics of mode coupling in the RBR. The dashed box indicates the tricoupler.

u_1 and u_2, respectively, indirectly coupled through a middle bus between each other. Because of the presence of a tricoupler at the coupling region, the mode decay in the RBR is quantitatively different compared with other traditional resonators based on a 2×2 coupler. The RBR has two main differences: there are two resonant modes (u_1 and u_2) that decay to the middle bus simultaneously (see upper inset) and the ring-bus coupling can induce an indirect coupling between the two outer rings through the tricoupler (see lower inset). We start by using the coupling of mode analysis to highlight the essential physics of the RBR and then present the EIT-like spectrum through integration of the RBR with MZI. As will be shown later, the TCMT is extraordinarily intuitive because it models the accurate positions where the transparency does occur. Finally, the TCMT is verified by its relationship with TMF and the experimental results.

2. Theoretical Analysis

For the RBR configuration loaded on the upper MZI arm in Fig. 1, the dynamic equations connecting the incoming wave (s_{in}), outgoing wave (s_{out}), and the resonance mode u (u_1 and u_2) in each individual ring can be modeled as [7]

$$du/dt = (i\Omega - \Gamma_i - \Gamma)u + iH^{T}s_{in}, s_{out} = s_{in} + iHu, \quad (1)$$

where Ω and Γ_i are 2×2 Hermitian matrices in which the diagonal elements represent the resonance frequencies and intrinsic loss, respectively. Γ is a Hermitian matrix describing the decay rates of two resonant modes to the middle bus and H is a matrix with elements of the ring–bus coupling coefficients. The expressions of u, Ω, Γ_i, and H are given by

$$u = \begin{bmatrix} u_1 \\ u_2 \end{bmatrix}, \quad \Omega = \begin{bmatrix} \omega_1 & 0 \\ 0 & \omega_2 \end{bmatrix}, \quad \Gamma_i = \begin{bmatrix} {\tau_{i1}}^{-1} & 0 \\ 0 & {\tau_{i2}}^{-1} \end{bmatrix},$$
$$H = \begin{bmatrix} \eta_1 \\ \eta_2 \end{bmatrix}^{T}, \quad \Gamma = \frac{1}{2}\begin{bmatrix} {\eta_1}^2 & \eta_1\eta_2 \\ \eta_1\eta_2 & {\eta_2}^2 \end{bmatrix}, \quad (2)$$

where the parameters with subscripts 1,2 correspond to the associated R1 and R2, respectively. The formula of the decay rate matrix Γ is obtained in the following way: the overall RBR system is energy conserving. We consider that the external incident wave is absent and there are finite amplitudes in the resonators at the initial time ($t = 0$). At $t > 0$, the resonant modes decay exponentially into the output port in terms of energy. Because of energy conservation in the overall RBR, power in the transmitted wave originates entirely from the decaying of the traveling modes, we have $d(u^*u)/dt = -2u^*\Gamma u = -{s_{out}}^* s_{out} = -u^*H^*Hu$. Thus, Γ can be expressed in terms of H as $\Gamma = H^*H/2$. In the expression of Γ, the diagonal elements ${\eta_{1,2}}^2/2$ are the decay rates of the corresponding resonant mode $u_{1,2}$ to the middle bus. The nonzero elements $\eta_1\eta_2/2$ are the indirect coupling between the two outer rings induced by the direct ring–bus coupling. Therefore, the two resonant modes form a nonorthogonal basis, because $\Gamma\Omega \neq \Omega\Gamma$ [8].

The parameters of TCMT in Eq. (2) are related to those of TMF by considering energy conservation and Q factor. For the former one, we assume that at the time of t, the resonators support traveling waves $u_{1,2}(t)$ with an amplitude of $U_{1,2}(t)$. Then $|u_{1,2}(t)|^2$ represents the total energy stored in the rings and $|U_{1,2}(t)|^2 = v_g {L_{1,2}}^{-1}|u_{1,2}(t)|^2$ stands for the entire power flowing through any cross section of the ring waveguides [2]. Considering that the power leaving the rings per round is equal to the change rate of energy in time domain, we have $|S_{out}|^2 = {t_1}^2|U_1(t)|^2 + {t_2}^2|U_2(t)|^2 = {\eta_1}^2|u_1(t)|^2 + {\eta_2}^2|u_2(t)|^2$, where $t_{1,2}$ represents the cross-coupling coefficients between of the two rings and the bus in the TMF. Between $t_{1,2}$ and r_0, there exists a relation of ${r_0}^2 + {t_1}^2 + {t_1}^2 = 1$ [11], if the loss-free coupling is assumed. Thus, the coupling coefficients in spatial and temporal formulations are related as ${\eta_{1,2}}^2 = {t_{1,2}}^2 v_g {L_{1,2}}^{-1}$. On the other hand, through solving the linewidth, i.e., the full width at half maximum (FWHM) of resonance in frequency ($\omega_{FWHM} = 2/{\tau_{i1,2}} + {t_0}^2$), the total Q factor (Q_t) can be calculated with the relation of the intrinsic loss and the coupling coefficient (${\eta_{1,2}}^2 = 2/\tau_{i1,i2}$) as ${Q_t}^{-1} = \omega_{FWHM}/\omega_{1,2} = {Q_i}^{-1} + {Q_e}^{-1} = \lambda_{FWHM}/\lambda_{1,2}$. $Q_i = (\tau_{i1,2}\omega_{1,2})/2$ is the intrinsic quality factor accounting for the ring absorption and $Q_e = (L_{1,2}\omega_{1,2})/({t_0}^2 v_g)$ is the external quality factor that is responsible for the ring-bus coupling. The notation λ_{FWHM} is the FWHM and $\lambda_{1,2}$ is the resonance wavelength of R1,2.

Solving Eq. (1) with Eq. (2) and the time dependence $s_{in} \sim \exp(i\omega t)$, we can arrive at the transmission of RBR (t_{RBR}). The transmission of a balanced MZI enhanced with RBR is then modeled by $t_{MZI} = i(t_{RBR} + 1)/2$,

$$t_{MZI} = \frac{i(i\Delta\omega_1 + {\tau_{i1}}^{-1})(i\Delta\omega_2 + {\tau_{i2}}^{-1})}{(i\Delta\omega_1 + {\tau_{i1}}^{-1} + {\eta_1}^2/2)(i\Delta\omega_2 + {\tau_{i2}}^{-1} + {\eta_2}^2/2) - {\eta_1}^2{\eta_2}^2/4}, \quad (3)$$

where $\Delta\omega_{1,2} = \omega - \omega_{1,2}$. The general transmission shape of Eq. (3) is plotted in Fig. 2 for two different conditions. We can see the RBR-MZI exhibit an EIT-like transmission feature that a narrow transparency peak occurs in the center of a broader transmission background, which is known as coupled-resonator-induced transparency (CRIT) [13].

The occurrence of the CRIT spectrum can be mathematically explained in the following procedure. For simplicity, we consider symmetric coupling ($\eta_1 = \eta_2$) and an identical intrinsic loss in the two rings ($1/\tau_{i1} = 1/\tau_{i2}$). In the case of $\eta_1{}^2/2 \gg |\omega_1 - \omega_2| \gg 1/\tau_{i1}$, there are two minima and a maximum at the positions $\omega = \omega_{1,2}$ and $\omega = (\omega_1 + \omega_2)/2$ in the transmission spectrum, respectively,

$$T_{\min} \equiv |t_{\mathrm{MZI}}|^2 \approx \frac{4\tau_{i1}{}^{-2}}{\eta_1{}^4},$$
$$T_{\max} \approx \frac{[(\omega_2 - \omega_1)/2]^4}{[\eta_1{}^2\tau_{i1}{}^{-1} - (\omega_2 - \omega_1)^2/4]^2}. \quad (4)$$

For the case when the widths $\Delta\omega_{1,2}$ are much less than the free spectral range of the cavity, i.e., $\Delta\omega_{1,2} \ll 2\pi v_g/L_{1,2}$, where $L_{1,2}$ and v_g are the perimeters of the two rings and the group velocity of the traveling mode, the transmission power of Eq. (4) at the ideal condition ($1/\tau_{i1,2} \sim 0$) can be rewritten as

$$T_{\mathrm{MZI}} = 1 - \frac{(2\eta_1{}^2)(2\eta_1{}^2)(\Delta\bar{\omega})^2}{(2\eta_1{}^2)^2(\Delta\bar{\omega})^2 + 4[(\Delta\bar{\omega})^2 - (\omega_2 - \omega_1)^2/4]^2}, \quad (5)$$

where $\Delta\bar{\omega} = \omega - (\omega_1 + \omega_2)/2$. We recall the EIT absorption expression (T_{abs}) in an atomic system [14] as $T_{\mathrm{abs}} = \Omega_1{}^2\Gamma\Delta^2/[\Delta^2\Gamma^2 + 4(\Delta^2 - \Omega_2{}^2/4)^2]$, where Ω_1 and Ω_2 are the respective Rabi frequencies of the probe field and the pump field. Γ is the decay rate and Δ is the detuning of the probe field from the atomic resonance. It can be seen that the fraction in Eq. (5) mimics the behavior of the EIT equation if we regard $\omega_2 - \omega_1 \sim \Omega_2$, $\Delta\bar{\omega} \sim \Delta$, and $2\eta_1{}^2 \sim \Omega_1$. From this analogy, we can see that no drive power is needed to generate transparency in the ring resonator system. The function of the powerful drive laser (Ω_1) used to create EIT in atomic vapor is realized by the interaction between the two rings ($2\eta_1{}^2$). It is worth noting that the bandwidth of the transparent resonance (Π) is arbitrarily narrow in the low-loss case:

$$\Pi \approx \frac{(\omega_2 - \omega_1)^2 + 4\tau_{i1}{}^{-2}}{2\eta_1{}^2 + (\omega_2 - \omega_1)}. \quad (6)$$

We can observe that the transparency becomes sharper with the increasing coupling strength η_1. This can be explained by the presence of nonorthogonal modes in the RBR structure, which renders a strong interaction between two rings. The transparency bandwidth can also be tuned by the separation of two resonance frequencies $|\omega_2 - \omega_1|$. The arbitrary transparency at $\omega = (\omega_1 + \omega_2)/2$ with a tunable bandwidth Π has several important potential applications. For instance, active tuning, e.g., switching, should be a promising application for the narrow CRIT resonance. Low-power switching can be realized in all-pass ring resonators, as shown in Fig. 2, where the transparency is shifted from the dashed curve to the solid curve. Using the perturbation theory calculation, a slight variation in the group index (n_g) of the larger ring ($\Delta n_g \sim 0.001$) can obtain 100% switching of the transparent frequency due to the Vernier effect of the two ring resonators [11]. In practice, fast switching speed and low-power consumption (or high extinction ratio) are the two important requirements in active optical devices. The CRIT used for switching with a high extinction ratio has been proposed in Ref. [9], but the switching speed of this CRIT has not yet been investigated. In fact, a trade-off exists between these two requirements. Taking the resonance of 1R1B as an example, in order to get low-power consuming modulation, a high-Q resonance is desirable. However, the higher Q leads to a longer effective cavity lifetime and lower optical losses, suggesting that more time must be taken by the resonator to maintain the same modulation depth [15]. This trade-off between the speed and power consumption can be broken by the high-Q transparency in the RBR-MZI with low ring finesse (or low cavity lifetime). The advantage of CRIT in RBR-MZI is that both requirements can be satisfied at a strong coupling condition, in contrast to a push–pull relation of the two requirements in conventional CRIT schemes or single-cavity resonators. Therefore, an active device with fast switching speed and low-power consumption can be realized using the CRIT in RBR-MZI.

We have introduced that the CRIT property can also be created in the similar configuration with two detuned PhC cavities [8] and two aperture-side-coupled FP cavities instead of rings [16]. However, in general, the RBR gives two separate resonances when the two resonances do not coincide with each other [11]. We believe that the mode analysis of the tricoupler in RBR-MZI is also helpful for analyzing the occurrence of induced transparency in the two similar devices. We take the transmission

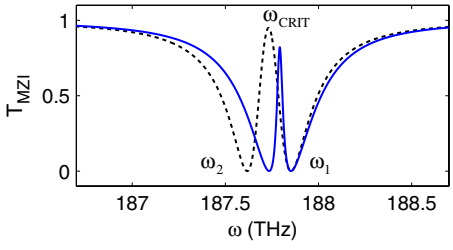

Fig. 2. (Color online) Transmissions of an RBR-MZI system. The transparent window occurs at $\omega = (\omega_1 + \omega_2)/2$ between ω_1 and ω_2. For the solid curve $\omega_2 - \omega_1 = 1.2$ GHz and for the dashed curve $\omega_2 - \omega_1 = 2.4$ GHz, where $Q_i/Q_e \approx 50$ is applied.

response of the PhC structure for example. Considering the standing wave with modified Eq. (1) and Eq. (2), e.g., $\Gamma = H^*H$, the normalized forward transmission (s_+/s_{in}) in such a PhC cavity can be obtained as

$$\frac{s_+}{s_{in}} = \frac{(i\Delta\omega_1 + {\tau_{i1}}^{-1})(i\Delta\omega_2 + {\tau_{i2}}^{-1})}{(i\Delta\omega_1 + {\tau_{i1}}^{-1} + {\eta_1}^2)(i\Delta\omega_2 + {\tau_{i2}}^{-1} + {\eta_2}^2) - {\eta_1}^2{\eta_2}^2}, \tag{7}$$

where all parameters have the same meanings as those in Eq. (2). Compared to Eq. (3), Eq. (7) has the remarkable similar expression except the modified decay rate terms (${\eta_{1,2}}^2/2$). This difference comes from the different working mechanisms of the two kinds of resonators, i.e., standing wave in a PhC cavity and traveling wave in a ring resonator. Therefore, in a PhC cavity, the resonant modes decay in both forward and backward directions, resulting in doubled decay rates between the middle waveguide and the two cavities. The CRIT spectrum described by Eq. (7) can also be explained by the bidirectional transmissions in PhC cavities. When the two resonance modes in the PhC cavities decay equally to the two output ports, the PhC system possesses nonorthogonal resonant modes, which results in the all-optical induced transparency analog of EIT in atomic systems [8].

3. Experimental Results

Figure 3(a) plots the fabricated RBR-MZI using silicon-on-insulator technology. Two 3 dB multimode interferometers with a width of 3.5 μm and a length of 11.5 μm are used to connect MZI arms. The 5 μm length tapers are used to connect input/output ports with the MZI arms to reduce the insertion loss. The first ring (R1) has a radius of 5 μm and a coupling length of 6 μm. The perimeter of the second ring (R2) is adjusted by the cavity size detuning γ, which is defined as the ratio of the circumferences of R1 and R2. Here in our design we set $\gamma = 1.05$ and the same coupling gap = 150 nm in both sides. Figure 3(b) shows the measurement result of the RBR-MZI transmission, which are fitted using Eq. (3) and the TMF [11]. In the curve fittings, $\gamma = 1.0468$, the loss factor $a = 0.995$ ($a = 1$ for lossless case), and the self-coupling coefficient for the middle waveguide $r_0 = 2r_{1,2} - 1 = 0.76$ are used. $r_{1,2}$ are the self-coupling coefficients of the R1,2, which are deduced from the fitting of add-drop resonators. Note that we still assume $r_1 = r_2$ for the RBR element because the radius difference (ΔR) between R1 and R2 is so small that the difference between r_1 and r_2 can be ignored, e.g., $\Delta R = 91$ nm. The MMI transmission factor ~0.88 is deduced from the measurement of a single multimode interference (MMI) device. In general, predictions from the two theoretical methods agree well with the measurement results. The asymmetry in the resonance comes from the nonzero self-coupling coefficient in the tricoupler [11] and the inevitable fabrication imbalance between the two MZI arms. This unwanted effect is compensated by a phase difference (0.35π) between the two MZI arms in the theoretical fittings. Figure 3(c) shows three measured transparent resonances with respect to the normalized wavelength λ. As expected, the linewidth of the transparency can be detuned individually for the two resonators.

The experimental results in Fig. 3(b) are obviously noisy compared to the simulated ones. One reason is that the measured devices suffer from some environmental effects, e.g., the moisture and dust, because the upper silicon cladding of the device has been removed. Another reason can be ascribed to the possible reflections between the grating couplers at both ends and the resonance between the two MMI couplers due to the high index contrast in the bare silicon devices [12]. Moreover, we need to point out that the TCMT is deduced from the coupled mode theory with the weak-coupling condition and perfect for very weak coupling, such as $r_1 > 0.99$ [1]. The slight difference between the two theoretical predictions comes in upon rather strong coupling, whereas the coupling strength is estimated as $r_1 = 0.88$ here. This difference can be reduced from optimizing the coupling conditions in the RBR component.

Furthermore, the experimental results tell us that the CRIT in RBR-MZI is created using two rings with the same intrinsic losses and self-coupling coefficients ($r_1 = r_2$), which is different from the two mutually coupled ring system [6,13], where the CRIT requires the losses in the two rings and the self-coupling coefficients to be different. A comparison between EIT-like expression of the RBR-MZI and that of the two mutually coupled ring configuration [6] reveals two main differences between the two systems. The first difference is that the bandwidth of the transparency is determined by the mutual coupling constant in the mutual coupled resonators, while it is

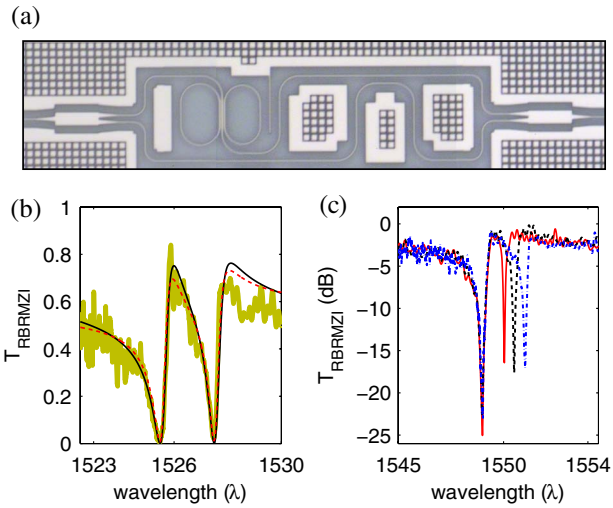

Fig. 3. (Color online) (a) Image of a fabricated RBR-MZI. (b) Measured (thick-faded curve), TMF (solid curve) and TCMT (dashed curve) transmissions of balanced arm length RBR-MZI. (c) CRIT with different linewidths.

determined by the detuning of resonance frequencies (or the separation of two resonances) in the RBR-MZI system $|\omega_2 - \omega_1|$. The second difference is that the CRIT only happens in the former system when the two resonant frequencies are coincident, whereas the later system requires the two rings to resonate at different frequencies.

4. Conclusion

A TCMT developed for the RBR configuration is applied for analyzing the CRIT generated in an RBR-MZI device. Mode analysis shows that the transparent resonance can be tuned by the coupling coefficients and frequency spacing. The TCMT calculation is consistent with that of TMF and the measurement results. The experiment results show that a CRIT resonance can be generated without requiring different losses in the two rings. This transparency enables applications for high-performance optical switching, where low power consumption and fast switching speed can be achieved.

This work was financially supported by the Singapore National Research Foundation (CRP award no. NRF-G-CRP 2007-01). T. Mei acknowledges financial support from the National Natural Science Foundation of China (grant no. 61176085), the Department of Education of Guangdong Province, China (grant no. gjhz1103), and the Bureau of Science and Information Technology of Guangzhou Municipality (grant no. 2010U1-D00131).

References

1. H. A. Haus, *Waves and Fields in Optoelectronics* (Prentice-Hall, 1984).
2. B. E. Little, S. T. Chu, H. A. Haus, J. Foresi, and J.-P. Laine, "Microring resonator channel dropping filters," J. Lightwave Technol. **15**, 998–1005 (1997).
3. L. Maleki, A. B. Matsko, A. A. Savchenkov, and V. S. Ilchenko, "Tunable delay line with interacting whispering-gallery-mode resonators," Opt. Lett. **29**, 626–628 (2004).
4. S. Kocaman, X. Yang, J. F. McMillan, M. B. Yu, D. L. Kwong, and C. W. Wong, "Observations of temporal group delays in slow-light multiple coupled photonic crystal cavities," Appl. Phys. Lett. **96**, 221111 (2010).
5. C. Manolatou and M. Lipson, "All-optical silicon modulators based on carrier injection by two-photon absorption," J. Lightwave Technol. **24**, 1433–1439 (2006).
6. Q. Li, T. Wang, Y. Su, M. Yan, and M. Qiu, "Coupled mode theory analysis of mode-splitting in coupled cavity system," Opt. Express **18**, 8367–8382 (2010).
7. S. Fan, W. Suh, and J. D. Joannopoulos, "Temporal coupled-mode theory for the Fano resonance in optical resonators," J. Opt. Soc. Am. A **20**, 569–572 (2003).
8. W. Suh, Z. Wang, and S. Fan, "Temporal coupled-mode theory and the presence of non-orthogonal modes in lossless multimode cavities," IEEE J. Quantum Electron. **40**, 1511–1518 (2004).
9. Q. Xu, "Silicon dual-ring modulator," Opt. Express **17**, 20783–20793 (2009).
10. A. W. Snyder, "Coupled-mode theory for optical fibers," J. Opt. Soc. Am. **62**, 1267–1277 (1972).
11. Y. Zhang, S. Darmawan, L. Y. M. Tobing, T. Mei, and D. H. Zhang, "Coupled resonator induced transparency in ring-bus-ring Mach–Zehnder interferometer," J. Opt. Soc. Am. B **28**, 28–36 (2011).
12. S. Darmawan, L. Y. M. Tobing, and D. H. Zhang, "Experimental demonstration of coupled-resonator-induced-transparency in silicon-on-insulator based ring-bus-ring geometry," Opt. Express **19**, 17813–17819 (2011).
13. D. D. Smith, H. Chang, K. A. Fuller, A. T. Rosenberger, and R. W. Boyd, "Coupled-resonator-induced transparency," Phys. Rev. A **69**, 063804 (2004).
14. Y. Li and M. Xiao, "Observation of quantum interference between dressed states in an electromagnetically induced transparency," Phys. Rev. A **51**, 4959–4962 (1995).
15. K. Preston, P. Dong, B. Schmidt, and M. Lipson, "High-speed all-optical modulation using polycrystalline silicon microring resonators," Appl. Phys. Lett. **92**, 151104 (2008).
16. Z. Han and S. I. Bozhevolnyi, "Plasmon-induced transparency with detuned ultracompact Fabry–Perot resonators in integrated plasmonic devices," Opt. Express **19**, 3251–3257 (2011).